https://doi.org/10.1093/plphys/kiac043 PLANT PHYSIOLOGY 2022: 189: 402–418

Plant Physiology®

Research Article

Brassinosteroids regulate rice seed germination through the BZR1-*RAmy3D* transcriptional module

Min Xiong [1], Jiawen Yu [1], Jindong Wang,[1] Qiang Gao [1], Lichun Huang [1,2], Chen Chen [2], Changquan Zhang [1,2], Xiaolei Fan,[1,2] Dongsheng Zhao,[1,2] Qiao-Quan Liu [1,2,†] and Qian-Feng Li [1,2,*,†]

1 Jiangsu Key Laboratory of Crop Genomics and Molecular Breeding/Jiangsu Key Laboratory of Crop Genetics and Physiology/Sate Key Laboratory of Hybrid Rice, College of Agriculture, Yangzhou University, Yangzhou 225009, Jiangsu, China
2 Co-Innovation Center for Modern Production Technology of Grain Crops of Jiangsu Province/Key Laboratory of Plant Functional Genomics of the Ministry of Education, Yangzhou University, Yangzhou 225009, Jiangsu, China

*Author for correspondence: qfli@yzu.edu.cn
†Senior authors.
These authors contributed equally (M.X., J.Y., J.W.).
Q.F.L., Q.Q.L., and M.X. conceived the project and designed the experiments. J.Y., J.W., L.H., and C.C. generated and analyzed the transgenic rice plants. M.X., J.Y., J.W., and Q.G. performed the other experiments. M.X., C.Z., X.F., D.Z., Q.Q.L., and Q.F.L. analyzed the data. M.X., Q.Q.L., and Q.F.L. wrote the manuscript. Q.Q.L, and Q.F.L. revised the manuscript.
The author responsible for distribution of materials integral to the findings presented in this article in accordance with the policy described in the Instructions for Authors (https://academic.oup.com/plphys/pages/general-instructions) is: Qian-Feng Li (qfli@yzu.edu.cn)

Abstract

Seed dormancy and germination, two physiological processes unique to seed-bearing plants, are critical for plant growth and crop production. The phytohormone brassinosteroid (BR) regulates many aspects of plant growth and development, including seed germination. The molecular mechanisms underlying BR control of rice (*Oryza sativa*) seed germination are mostly unknown. We investigated the molecular regulatory cascade of BR in promoting rice seed germination and post-germination growth. Physiological assays indicated that blocking BR signaling, including introducing defects into the BR-insensitive 1 (BRI1) receptor or overexpressing the glycogen synthase kinase 2 (GSK2) kinase delayed seed germination and suppressed embryo growth. Our results also indicated that brassinazole-resistant 1 (BZR1) is the key downstream transcription factor that mediates BR regulation of seed germination by binding to the *alpha-Amylase 3D* (*RAmy3D*) promoter, which affects α-amylase expression and activity and the degradation of starch in the endosperm. The BZR1-*RAmy3D* module functions independently from the established Gibberellin MYB-*alpha-amylase 1A* (*RAmy1A*) module of the gibberellin (GA) pathway. We demonstrate that the BZR1-*RAmy3D* module also functions in embryo-related tissues. Moreover, RNA-sequencing (RNA-seq) analysis identified more potential BZR1-responsive genes, including those involved in starch and sucrose metabolism. Our study successfully identified the role of the BZR1-*RAmy3D* transcriptional module in regulating rice seed germination.

Introduction

Seed dormancy and germination, two distinct physiological processes that are characteristic of seed-bearing plants, are critical for both plant development and crop production. Successful seed germination is an important beginning for the next round of the plant life cycle, and thus leads to

Received September 02, 2021. Accepted January 07, 2022. Advance access publication February 9, 2022

robust and healthy seedling development and thus high yielding crops. Seed germination begins with the absorption of water and ends with the protrusion of the radicle. Suitable temperatures and sufficient availability of water and oxygen are the prerequisites for normal germination (Holdsworth et al., 2008). Once the seeds begin to germinate after water absorption (imbibition), seed storage reserves, including starch and storage proteins, are degraded by various hydrolytic enzymes and then converted into energy and nutrients for radicle protrusion and subsequent seedling growth. In rice (*Oryza sativa*) seed germination, the carbon source needed for the early heterotrophic embryo (the sink) is completely dependent on the carbohydrate reserve in the endosperm (the source; Scofield et al., 2007). Starch, as the primary source of carbohydrate during germination, plays an important role in the source–sink communication. In cereal endosperms, the degradation of starch into glucose requires a number of enzymes, including α-amylase, β-amylase, limit dextrinase (LDA), and maltase (Zeeman et al., 2010). Briefly, α-amylase attacks starch granules to release branched and linear glucose polymers, which are then transformed into the linear glucans by LDA. Subsequently, α-amylase and β-amylase further catalyze the degradation of linear glucans into glucose, which is then used for embryo growth (Noronha et al., 2018). In barley (*Hordeum vulgare*), during the gradual degradation of seed starch, size of the surface pores of the starch granule are increased, and internal erosion and disintegration of the granules are intensified (Andriotis et al., 2016).

As a pivotal enzyme that catalyzes the degradation of starch in cereal seeds, α-amylase has been reported to be closely related to multiple key agronomic traits, such as germination rate (Asatsuma et al., 2005), seedling vigor (Karrer et al., 1992), and hypoxia stress (Hwang et al., 1999). In cereals, the α-amylase family contains a number of members. For example, there are 10 members in rice (Damaris et al., 2019), 12 in barley (Zhang and Li, 2017), and 22 in wheat (*Triticum aestivum*; Huang et al., 1992). Based on the sequence polymorphism of α-amylase genes, they can be divided into two major groups in rice, *AmyA* and *AmyB*. The *AmyA* group is further subdivided into the *Amy1* and *Amy2* subfamilies, and the *AmyB* group includes the *Amy3* subfamily (Huang et al., 1992). The members of these subfamilies are designated *alpha-amylase 1A* (*RAmy1A*), *RAmy1B*, *RAmy1C*, *RAmy2A*, *RAmy3A*, *RAmy3B*, *RAmy3C*, *RAmy3D*, *RAmy3E*, and *RAmy3F*. Except for *RAmy3F*, most α-amylase genes have been experimentally verified. Regulating the expression of α-amylase genes is a common strategy by which plants coordinate growth and development. Multiple conserved cis-elements in the α-amylase gene promoters are crucial for this regulation. For example, gibberellin (GA) activates α-amylase expression through the GA response complex (GARC) motif (Lanahan et al., 1992). GARC includes two closely correlated components, namely the GA response element (GARE) and TA box (Chen et al., 2006). Gibberellin MYB (GAMYB), a GA-induced key transcription factor, binds directly to GARE and positively regulates the expression of a series of hydrolase genes, including amylase genes (Gubler and Jacobsen, 1992; Washio, 2003). In barley, abscisic acid (ABA) antagonizes GA by inhibiting GAMYB expression and subsequent α-amylase expression, thus modulating seed dormancy and germination (Gómez et al., 2001). Under conditions of sugar starvation, a transcription factor called MYBS1 is induced and interacts with the TA box in the *RAmy3D* promoter, thus promoting seed germination (Lu et al., 2007). Moreover, GA promotes the co-nuclear transport of GAMYB and MYBS1 to form the (MYBS1-GAMYB)-DNA (GARE-TA box) complex, which induces amylase gene expression (Hong et al., 2012). Therefore, the two MYB transcription factors play key roles in coordinating the expression of α-amylase by sugars and GA. There are also other abiotic factors that directly or indirectly regulate seed germination, such as salinity (Liu et al., 2018). In addition, chemicals, such as maleic hydrazide, eugenol, and uniconazole reduce the expression of *RAmy3B* and *RAmy3E* in hybrid rice seeds, thus preventing pre-harvest sprouting (PHS; Hu et al., 2016). PHS is one of the most severe problems affecting rice production that causes reductions in rice yield, grain quality, and seed vitality. Therefore, α-amylase genes are crucial determinants of both seed germination and PHS.

Although considerable progress has been made in understanding how GA and ABA regulate seed germination and dormancy, the mechanisms by which the other phytohormones modulate these processes are still mostly obscure. For example, brassinosteroids (BRs), a major class of growth promoting phytohormones, are also involved in regulating seed germination (Tong and Chu, 2018; Li et al., 2020). In Arabidopsis (*Arabidopsis thaliana*), BR promotes seed germination via antagonizing the suppression effect of ABA, mechanistically by targeting ABSCISIC ACID-INSENSITIVE5 (ABI5), a key component in ABA signaling pathway (Hu and Yu, 2014; Zhao et al., 2019). Moreover, BR and GA co-induce seed germination via activating *GASA6* in Arabidopsis (Zhong et al., 2021). Further dissecting the mechanism of action of BRs in rice germination will not only advance our understanding of BR signaling in crops, but also boost its future application in rice breeding programs. Considering that BRs play multifaceted roles in several key agronomic traits of rice, optimizing the manipulation of these hormones for desired beneficial traits without adverse effects is vital to their practical application in agriculture. In general, rice shares a similar primary BR signaling pathway with Arabidopsis. In brief, the BR signal is sensed by the BR insensitive 1 (OsBRI1) receptor and the BRI1-associated receptor kinase 1 (OsBAK1) coreceptor which triggers a series of downstream phosphorylation events, including the activation of BR-signaling kinase 3 (OsBSK3) kinase and the suppression glycogen synthase kinase 2 (GSK2) kinase activity (Tong and Chu, 2018). OsGSK2, a GSK3/SHAGGY-like kinase homologous to BR-

insensitive 2 (BIN2) in Arabidopsis, acts as the central negative regulator of the BR signaling pathway by phosphorylating and inactivating the downstream transcription factors, including brassinazole-resistant 1 (OsBZR1) and dwarf and low-tillering (DLT; Bai et al., 2007; Tong et al., 2012). At present, it is still unclear whether starch, the most abundant seed storage reserve, is also involved in BR-regulated rice germination. The underlying molecular mechanism remains to be discovered. In this study, we describe a novel regulatory module of seed germination, from the BR receptor to the downstream key transcription factor BZR1 and its specific target genes, and we highlight the central roles of the new BZR1-*RAmy3D* module in starch mobilization.

Results

BR signaling promotes seed germination and post-germination growth

To determine whether BR-signaling affects seed germination in rice, a number of BR-related rice and mutant lines were used in a germination assay, including *d61* and its wild-type Taichung 65 (TC65), *Go*, *dlt*, *Do*, and their wild-type Zhonghua 11 (ZH11). Since various BR mutants were produced in different recipient rice varieties, specific wild-type should be used as the control for corresponding BR mutants in various experiments. *d61* is a mild BR-insensitive mutant with a defect in the BR receptor BRI1 (Yamamuro et al., 2000), whose plant height, grain size, and 1,000-grain weight were all significantly declined (Supplemental Figure S1, A–F). *Go* is a transgenic rice line that overexpresses *GSK2* (Tong et al., 2012). Similarly, its plant height, grain size, and 1,000-grain weight were also all decreased (Supplemental Figure S1, G–L). In addition, *dlt* and *Do* are the *DLT* mutant and overexpression lines, respectively (Tong et al., 2012). Interestingly, plant height in both the *Do* overexpression lines and *dlt* mutant was decreased compared to the wild-type (Supplemental Figure S1M). Moreover, the grain length of rice *Do* was increased, while its grain width was decreased; the change of grain length and width of *dlt* mutant was opposite to that of *Do* (Supplemental Figure S1, N–R). The result of germination assay showed that the BR receptor mutant *d61* was ~12 h slower than the wild-type control to reach 100% germination (Figure 1A). Moreover, the shoot lengths of the germinating *d61* seeds were shorter than those of the wild-type (Figure 1B; Supplemental Figure S2). As expected, the germination rate and shoot length of seeds from plants overexpressing *OsGSK2* (*Go*) were similar to those of the *d61* mutant (Figure 1, C and D). However, both the overexpression line (*Do*) and the mutant (*dlt*) of *DLT*, a GSK2-regulated transcription factor that is important in the BR signaling pathway, showed no observable differences in seed germination compared with the wild-type (Figure 1, E and F). Therefore, BR positively regulates seed germination and embryo growth, but the regulation is not mediated by the transcription factor DLT.

The *bzr1* mutant shares similar germination features with *d61*

In addition to DLT, OsBZR1 is another key transcription factor in the BR signaling pathway. Therefore, we further tested whether it is OsBZR1 that connects the upstream BR signal with the downstream specific target genes that control seed germination. First, we generated *OsBZR1* overexpression (*BZR1-OX*) and knockout (*bzr1*) lines under the genetic background of the *japonica* cultivar Nipponbare (Nip). Gene expression analysis indicated that *OsBZR1* expression was notably increased in seeds of the overexpression lines (Figure 2A). Western blotting further confirmed that the BZR1-3XFLAG fusion protein was successfully expressed in the test lines (Figure 2B). Further pharmacological analyses showed that the BZR1 protein abundance slightly decreased in response to brassinazole (BRZ) treatment, a BR biosynthesis inhibitor (Figure 2C). While brassinolide (BL) treatment notably induced the dephosphorylation of BZR1, thus activating the BR signaling pathway (Figure 2D). As for the *bzr1* mutants generated via clustered regularly interspaced short palindromic repeats/CRISPR associated protein 9 (CRISPR/Cas9) genome editing, DNA sequencing showed that two homozygous mutants were obtained, *bzr1-i1* and *bzr1-d4*, which resulted from a one basepair (bp) insertion and a 4-bp deletion in the first exon, respectively (Figure 2E).

We next examined several important agronomic traits of the *OsBZR1*-related rice lines, including plant height, grain size, and 1,000-grain weight. Plant height in both the *OsBZR1* overexpression and knockout lines was slightly decreased compared to the control (Supplemental Figure S3, A and B), which is similar to that in *DLT* mutant and overexpression rice (Supplemental Figure S1M; Tong et al., 2009, 2012). We hypothesize that the reduction of plant height in *OsBZR1* and *DLT* overexpression lines should be due to the dose-dependent effect of BR on cell elongation, that is low concentrations of BR increase while high concentrations of BR often reduce plant height (Tong et al., 2014). As to grain size, no change was observed in the *OsBZR1-OX* line, but the length, width, and thickness of *bzr1* mutant grains were all slightly reduced (Supplemental Figure S3, C–F). Hence, the 1,000-grain weight of the *bzr1* mutants were reduced by 7%–8% compared to the wild-type, while the *BZR1-OX* grains were not significantly different (Supplemental Figure S3, C–G). Moreover, *bzr1* seedling height was also reduced compared to wild-type, while that of *BZR1-OX* seedlings was not (Supplemental Figure S4). Next, the lamina joint inclination test was performed to examine the leaf angles of *BZR1*-related materials, which is the most distinctive BR-responsive architectural trait in cereals. Ample evidence demonstrates that the leaf angles of BR-deficient or -insensitive mutants are reduced while that of BR-treated rice is increased (Sakamoto et al., 2006; Tong et al., 2012; Sun et al., 2015). The test result showed that although the leaf angle in

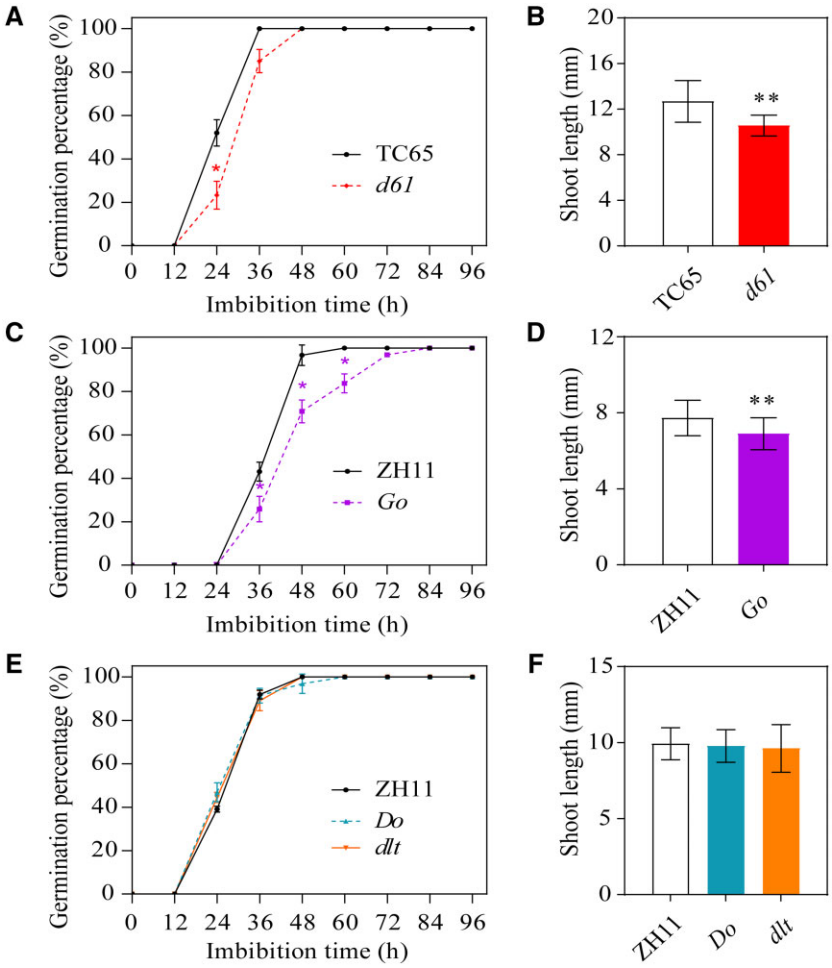

Figure 1 Germination analysis of BR-insensitive mutant seeds. A–F, Germination rate from 0 to 96 HAI and shoot length at 96 HAI in *d61* and wild-type TC65 seeds (A and B), *Go* and wild-type ZH11 seeds (C and D), and *Do*, *dlt*, and ZH11 seeds (E and F). Error bars represent SD ($n = 3$ experiments, each replicate contained 30 seeds). *$P < 0.05$; **$P < 0.01$ (Student's *t* test).

BZR1-OX seedlings was unchanged, the leaf angles of the *bzr1* mutants was smaller than in the wild-type, both with or without BR treatment (Figure 2, F and G), indicating that knockout of *OsBZR1* expression reduces seedling leaf angle and BR sensitivity. Since rice plants with erect leaves (small leaf angle) can improve grain yield per unit area in dense planting populations (Sinclair and Sheehy, 1999), *bzr1* mutants may have the potential to enhance rice grain yield.

In addition, germination of the *bzr1* mutant seeds was delayed, while that of *BZR1-OX* seeds was essentially unchanged compared to the control (Figure 2H). In more detail, the dynamic germination pattern of the *bzr1* mutants was similar to that of the *d61* mutant and the *OsGSK2* overexpression line; both took at least 12-h longer than the wild-type to reach 100% germination (Figure 1, A and C). Moreover, shoot length in the *bzr1* mutants was also significantly reduced (Figure 2I; Supplemental Figure S5). Most importantly, PHS in the *bzr1* mutants was less severe than in the wild-type under conditions of high temperature and humidity (Figure 2, J and K). The germination rates of the *bzr1* mutants were notably lower than in the wild-type at each time-point examined (Figure 2L), and the shoot lengths were also shorter in the *bzr1* mutants (Figure 2K). Therefore, although mutations in *OsBZR1* cause a 12-h delay in seed germination and a slight reduction in shoot length, their effect on enhancing PHS tolerance in rice was substantial.

BR signaling enhances starch mobilization in germinated seeds

Since α-amylase and starch mobilization play important roles in regulating seed germination, we investigated whether BZR1 also regulates seed germination in this way. Thus, α-amylase activity in the BR-related rice lines was determined qualitatively and quantitatively. First, starch plate test was performed for evaluation of the α-amylase activity. In more detail, the embryo-less half-seeds can synthesize and secrete α-amylases for degradation of starch, thus producing the colorless halo around the seed. Therefore, the halo size positively corresponds to α-amylase activity of seeds. The results of starch plate test showed that the clear zones around *d61*, *Go*, and *bzr1* seeds were smaller than the zones around seeds from their respective wild-types

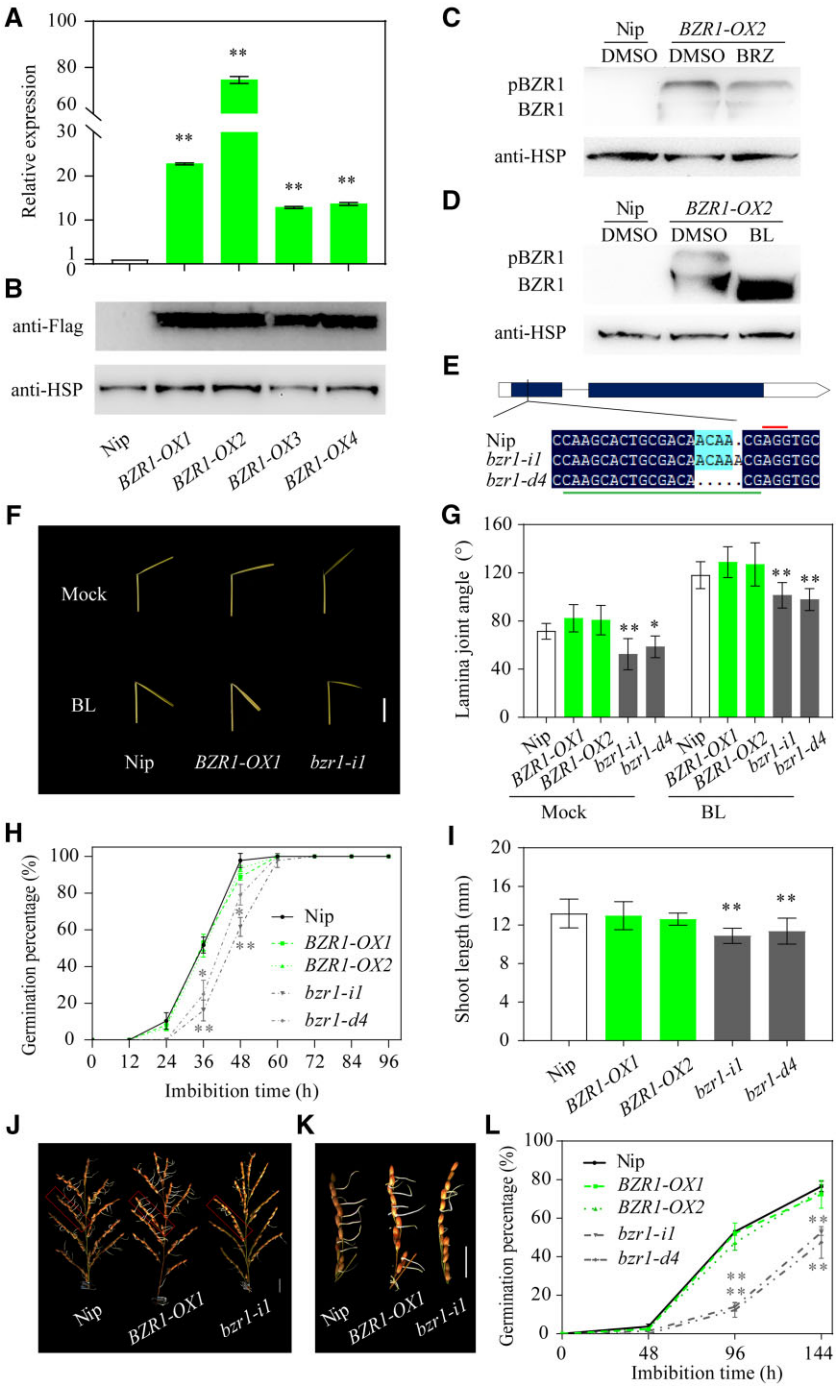

Figure 2 Germination of transgenic *BZR1-OX* and *bzr1* mutant rice seeds. A, Expression of *BZR1* in the seeds of four *OsBZR1-OX* lines and "Nip". *Actin1* was used as the internal control for normalization of gene expression data. B, Expression analysis of BZR1-3XFlag fusion protein in the leaves of *OsBZR1-OX* rice seedlings. C, Effect of BRZ (2 μM) treatment on the abundance of BZR1-3XFlag. The 5-d-old seedlings were grown in water supplemented with 2-μM BRZ or DMSO mock for another 5 d. BRZ, a specific BR biosynthetic inhibitor. D, Effect of BL (1 μM) treatment on the phosphorylation status of BZR1-3XFlag. The leaves of 10-d-old rice seedlings were treated with 1-μM BL or DMSO for 3 h in vitro. BL, the most active BR. Detection of heat shock protein (HSP) was used as the reference for protein loading. BZR1-3XFlag and HSP proteins were detected with antibodies directed against the 3XFlag tag epitope and HSP, respectively. E, Schematic diagram of the target sequence for *OsBZR1* gene editing and the sequences of the two *bzr1* mutants generated using CRISPR/Cas9. *bzr1-i1* and *bzr1-d4* have a 1-bp insertion and a 4-bp deletion, respectively, in the *OsBZR1* target site (underlined in green). The 5′-AGG-3′ protospacer-adjacent motif is marked with a red line. F, BL sensitivity test of *BZR1-OX1*, *bzr1-i1*, and wild-type seedlings using the lamina joint inclination assay. Scale bar = 1 cm. G, Quantitative analysis of the lamina joint inclination assay data as described in (F). Error bars represent SD (n = 3 experiments, each replicate contained 20 seedlings). H and I, Germination rate (H) and shoot length at 96 HAI (I) of germinated *BZR1-OX1*, *bzr1-i1*, and wild-type Nip seeds. J and K, PHS phenotypes of mature rice panicles (J) and spikelets (K) of *BZR1-OX1*, *bzr1-i1*, and the wild-type after 6 d of imbibition in water. Scale bar = 2 cm. L, Time-course analysis of seed germination rates of the panicles from wild-type, two *BZR1-OX* lines, and two *bzr1* mutants. Error bars represent SD (n = 3 experiments, each replicate contained 30 seeds or 10 panicles). In this figure, $^*P < 0.05$; $^{**}P < 0.01$ (Student's t test). The images were digitally extracted for comparison in panels F, J, and K.

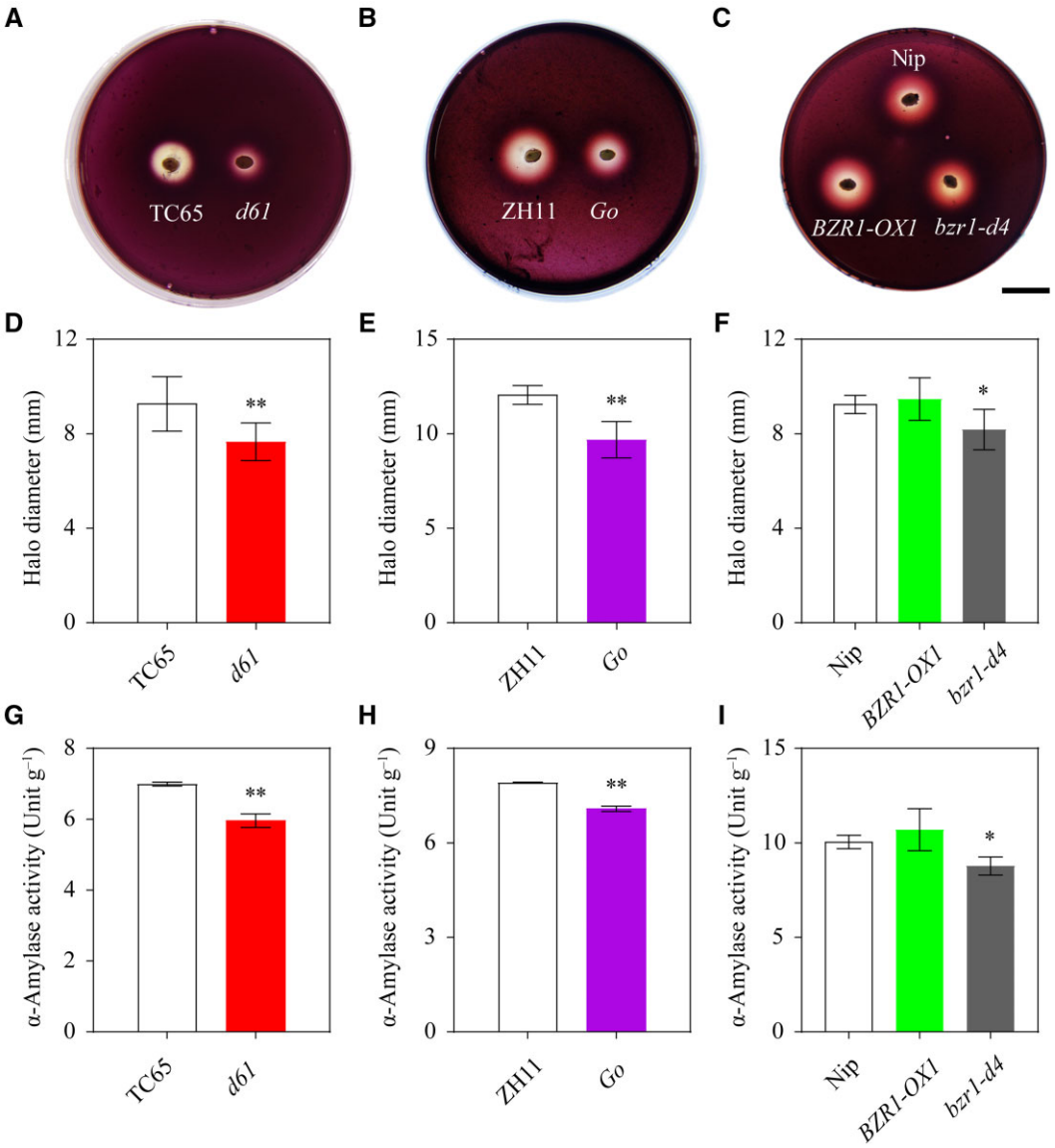

Figure 3 Analysis of α-amylase activity in BR signaling-related rice lines. A–C, Representative images of qualitative comparisons of α-amylase activity between BR signaling-related rice lines and their corresponding wild-types at 96 HAI in the starch plate test. Scale bar = 10 mm. D–F, Quantitative analysis of the halo diameters in the starch plate test. G–I, Quantitative analysis of α-amylase enzyme activity data in the rice samples at 96 HAI. Error bars represent SD (n = 3 experiments, each replicate contained 30 seeds). *$P < 0.05$; **$P < 0.01$ (Student's t test).

(Figure 3, A–F; Supplemental Figure S6, A and B), suggesting that less α-amylase was produced in these seeds during germination. Next, we directly measured the α-amylase activity of the germinating seeds, and the results were consistent with those of the starch plate test (Figure 3, G–I; Supplemental Figure S6C), implying that reduced α-amylase activity could be one important reason for the delayed germination in seeds of BR-insensitive rice.

To further confirm our hypothesis that BR regulates α-amylase activity and that starch degradation affects seed germination, we measured the contents of total starch and soluble sugar of the different BR-insensitive mutants. The results showed that blocking BR signaling indeed reduces the degradation of total starch (Supplemental Figure S7, A–C) and results in less soluble sugar contents in the germinating seeds at 96 h after imbibition (HAI; Supplemental Figure S8, A–C), which is consistent with above α-amylase activity test. Although the soluble sugar content of *Go* seeds was higher than in the wild-type before germination, after 96 h of imbibition, the soluble sugar content of the *Go* seeds was lower (Supplemental Figure S8B). These findings suggest that BRs likely fine-tune seed germination by regulating the conversion efficiency of stored starch to soluble sugar.

OsBZR1 directly regulates *RAmy3D* expression

To further determine which α-amylase family member directly connects the BR pathway and endosperm starch degradation, we examined the expression of rice α-amylase genes. First, we evaluated *BZR1* expression at different time

points during seed germination. The results showed that *BZR1* transcription is highest at the initial stage of seed imbibition (2 HAI) followed by a sharp decline at 24 HAI, after which it gradually increased and reached a second peak at 72 HAI (Supplemental Figure S9). Considering the essential role of α-amylase in the first step of starch degradation and that *BZR1* expression was the highest at 2 HAI, we examined the transcription of all reported α-amylase genes in the seeds at 2 HAI. In general, the expression of *RAmy3D* was the highest in the early stage of seed germination (Figure 4, A and B). In *d61*, the expression of *RAmy3D* was downregulated, while the expression of three other family members with moderate expression levels varied; *RAmy3E* expression was also downregulated while *RAmy3A* and *RAmy1A* were upregulated (Figure 4A). In addition, *RAmy3D* had a much larger expression change in BZR1-related rice lines than in the *d61* mutant, with an increase in *BZR1-OX* seeds and a decrease in the *bzr1-i1* mutant (Figure 4B). Furthermore, we also monitored the expression pattern of *RAmy3D* during seed germination. Interestingly, its expression pattern was somewhat similar to that of *BZR1*; that is, its highest expression occurs at the initial stage of seed germination (Supplemental Figure S10). Based on these data, we hypothesized that *RAmy3D* could be the potential target of BZR1 that is responsible for BR-regulated starch degradation during seed germination.

To further confirm this notion, a dual-luciferase reporter approach was used to test how BZR1 regulates *RAmy3D*. The promoter of *RAmy3D* was fused with LUC to generate a reporter plasmid, and the 35S::*BZR1* construct was used as the effector (Supplemental Figure S11). Consistent with our previous results, *BZR1* overexpression significantly upregulated the expression of *LUC* driven by the *RAmy3D* promoter (Figure 4C). Considering that BZR1 is an important transcription factor that can directly bind to the BR response element (BRRE) elements and E-box in the target gene promoters (He et al., 2005), we analyzed the *RAmy3D* promoter for potential OsBZR1 binding sites. We identified a total of five E-box motifs in the 2-kb region upstream of the *RAmy3D* transcription start site (Figure 4D). Hence, specific primers were designed to confirm the direct binding of BZR1 to these motifs using the chromatin immunoprecipitation ChIP quantitative polymerase chain reaction (ChIP-qPCR) assay. This analysis indicated that all five test regions were enriched, with the highest enrichment in the P3 and P4 regions (Figure 4E). To further verify the direct binding of BZR1 to the *RAmy3D* promoter, we performed an electrophoretic mobility shift assay (EMSA). Here, the P3 and P4 regions were selected for analysis due to their high level of enrichment in the ChIP-qPCR assay. Unsurprisingly, the EMSA result showed that maltose binding protein (MBP)–BZR1 directly interacts with both the P3 and P4 promoter regions (Figure 4F; Supplemental Figure S12). As the amount of unlabeled competitor probes increased, the BZR1-labeled probe complexes were gradually eliminated (Figure 4F; Supplemental Figure S12). Therefore, we conclude that OsBZR1 regulates *RAmy3D* expression by directly binding to its gene promoter.

The BZR1-*RAmy3D* module is independent of the GAMYB-*RAmy1A* module

GA can activate the GAMYB transcription factor and enhance its binding to the GARE motif in the *RAmy1A* promoter, thus promoting its expression (Washio, 2003). Because it is well-known that BR interacts with GA to coordinate multiple plant growth and developmental events, it will be interesting to determine whether they also show crosstalk in modulating starch mobilization and the subsequent seed germination. Therefore, a dual luciferase reporter analysis was performed, and the results confirmed that GAMYB promoted the expression of *LUC* driven by the *RAmy1A* promoter, whereas BZR1 did not (Figure 5A; Supplemental Figure S11). In contrast, the promotion effect of GAMYB on the *RAmy3D* promoter was not significant (Figure 4C). These data imply that BR regulates starch degradation via the specific BZR1-*RAmy3D* module, while GA acts through the particular GAMYB-*RAmy1A* module. Interestingly, although three E-boxes and one BRRE element are present in the *RAmy1A* promoter (Figure 5B), the ChIP-qPCR result showed no enrichment of these regions (Figure 5C). Moreover, *RAmy1A* exhibited a different expression pattern to *RAmy3D* (Supplemental Figure S13). In addition, *RAmy3D* is not the target of GAMYB because it lacks the GARE motif. Correspondingly, its transcription is not regulated by GAMYB based on the result of dual luciferase reporter assay (Hong et al., 2012; Figure 4C). Furthermore, BZR1 did not directly interact with GAMYB (Figure 5D). Therefore, BZR1-*RAmy3D* and GAMYB-*RAmy1A* appear be two independent regulatory modules that control α-amylase gene expression and starch degradation.

We also evaluated the sensitivity of *bzr1-i1* to GA and paclobutrazol (PAC), a GA biosynthesis inhibitor, during seed germination (Figure 5E). The data from this experiment showed that GA treatment promoted while PAC treatment delayed seed germination of both Nip and the *bzr1* mutant when compared with their respective ethanol-treated controls (Figure 5F). On the other hand, the *bzr1* mutant always germinated slower than the wild-type under the same germination conditions, either with GA, PAC, or mock treatment (Figure 5F). Moreover, GA only partially restored, whereas PAC further aggravated, the suppressive effect of the *bzr1-i1* mutation on shoot elongation (Figure 5, E and G). The above data suggest that BZR1-regulated seed germination is at least partially independent of GA.

BR promotes shoot elongation by increasing the degradation of transient starch in the embryo

Considering that *RAmy3D* promoted starch degradation is correlated with the release of energy for shoot elongation under anoxic conditions (Damaris et al., 2019), we further investigated whether the BZR1-*RAmy3D* module is also directly involved in rice shoot elongation. Since bending in

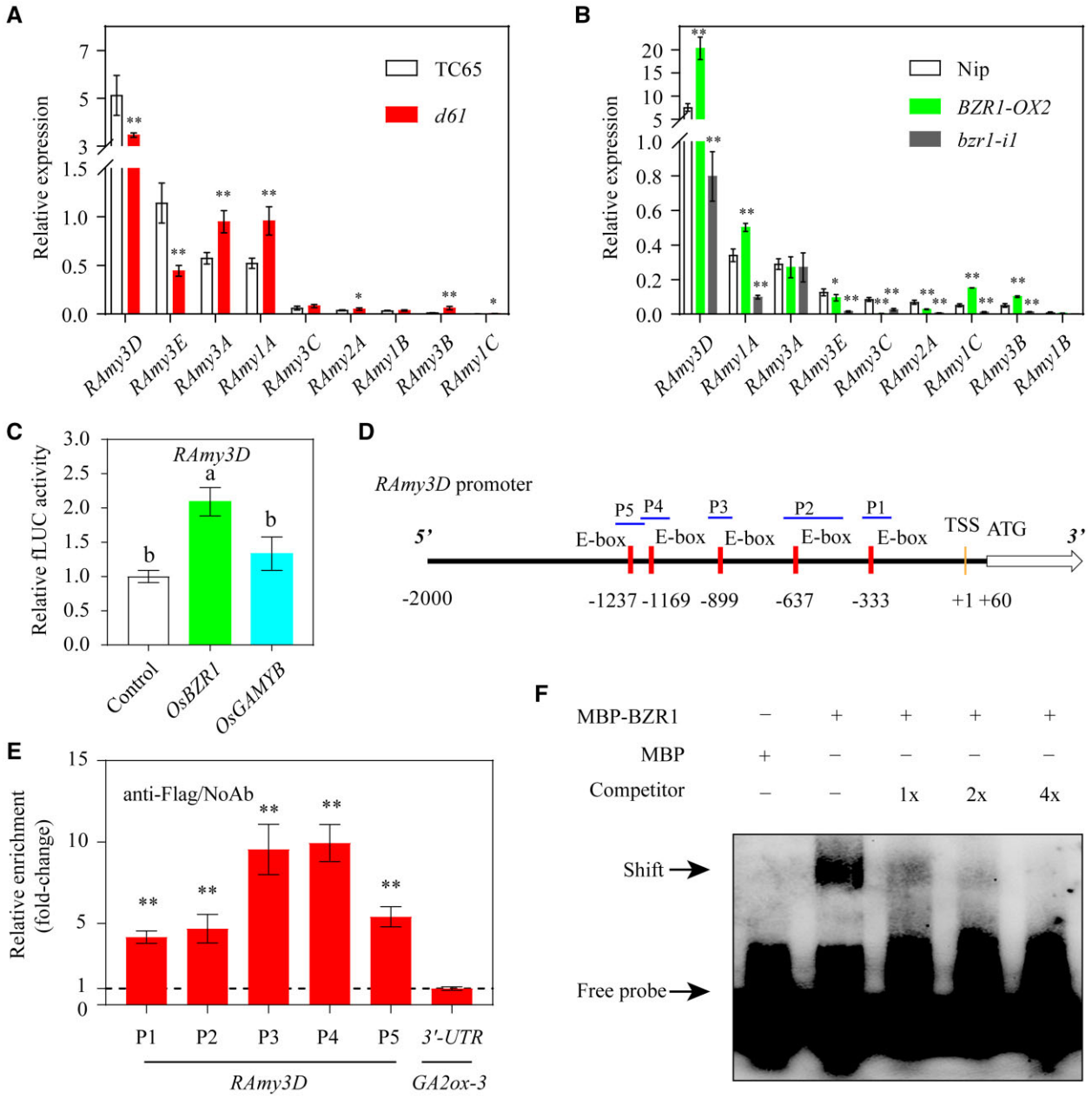

Figure 4 OsBZR1 binds directly to the promoter of *RAmy3D* and activates its expression. A, RT-qPCR analysis of nine α-amylase family genes in seeds of the *d61* mutant and the wild-type TC65 at 2 HAI. B, RT-qPCR analysis of the α-amylase family genes in the seeds of *BZR1-OX* and the *bzr1-i1* mutant and the wild-type Nip at 2 HAI. In A and B, *Actin1* was used as the internal gene expression control. Error bars represent SD ($n = 3$ experiments). *$P < 0.05$; **$P < 0.01$ (Student's *t* test). C, BZR1, but not GAMYB, activates the *RAmy3D* promoter. The relative activation values are shown by the LUC/REN ratios. The LUC/REN value for the empty vector plus *RAmy3D* promoter reporter control sample was set to 1. LUC, firefly luciferase; REN, renilla luciferase. Error bars represent SD ($n = 6$ experiments). Different letters indicate significant differences at $P < 0.05$ by Duncan's multiple range test. D, Distribution of five BZR1-binding E-box motifs in the 2-kb region upstream of the *RAmy3D* transcription start site (TSS). The P1 to P5 regions marked with blue lines represent the positions used for the ChIP-qPCR assay. E, Relative enrichment of the OsBZR1 binding sites compared with the samples without antibody (NoAb) determined by the qPCR assay. All values were normalized to an unrelated *Actin1* intron region, and a DNA fragment from the 3′ untranslated region (UTR) of *GA2ox-3* was used as the negative control (Tong et al., 2014). Error bars represent SD ($n = 3$ experiments). **$P < 0.01$ (Student's *t* test). F, OsBZR1 binding to the P4 region of the *RAmy3D* promoter shown in an EMSA. The MBP–BZR1 recombinant protein was mixed with the labeled P4 probe together with different amounts of the unlabeled probe as competitor. – or + represent the absence or presence of the indicated components, respectively. The first lane without MBP–BZR1 protein did not cause a mobility shift in the labeled probe.

growing shoots is often caused by the unequal growth of cells on opposite sides, we examined the faster and slower growing sides of the shoots, which we called the outside and inside parts, respectively. Interestingly, more transient starch granules were found to accumulate in the inside cells compared to the outside cells (Figure 6, A–N), implying that

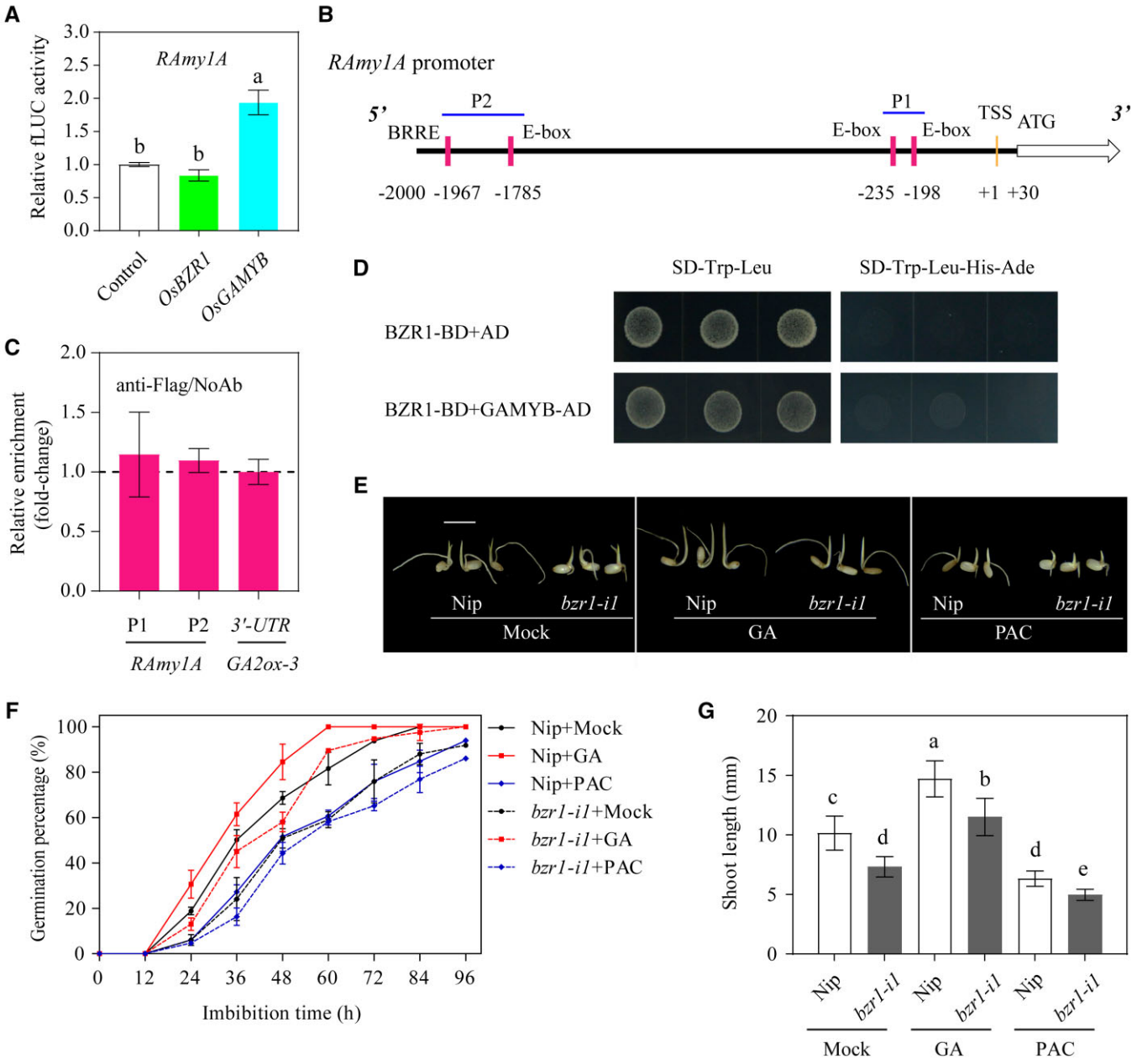

Figure 5 The BZR1-*RAmy3D* transcriptional module is independent of the established GAMYB-*RAmy1A* module. A, GAMYB, not BZR1, activates transcription in the *RAmy1A* promoter. The relative activation is shown by the LUC/REN ratio. The LUC/REN value of the empty vector plus the *RAmy1A* promoter reporter control sample was set to 1. LUC, firefly luciferase; REN, renilla luciferase. Error bars represent SD (n = 3 experiments). Different letters indicate significant differences at $P < 0.05$ by Duncan's multiple range test. B, Distribution of three E-box motifs and one BRRE in the 2-kb region upstream of the *RAmy1A* transcription start site (TSS). The P1 and P2 regions marked with blue lines represent the position of the DNA fragments used for the ChIP-qPCR assay. C, Relative enrichment of the OsBZR1 binding sites compared with the samples without antibody (NoAb) determined by qPCR assay. All values were normalized to an unrelated *Actin1* intron region, and a DNA fragment located in the 3′–untranslated region (UTR) of *GA2ox-3* was used as the negative control (Tong et al., 2014). Error bars represent SD (n = 3 experiments). D, BZR1 does not directly interact with GAMYB in a yeast two-hybrid assay. The empty *pGADT7* (AD) vector was used as the negative control. E, Morphology of germinating seeds at 96 HAI of the *bzr1* mutant and the Nip wild-type treated with gibberellin (GA, 10 μM), paclobutrazol (PAC, 10 μM), or the ethanol mock treatment. PAC is a GA biosynthesis inhibitor. Scale bar = 10 mm. F and G, Germination rate (F) and shoot length at 96 HAI (G) in germinated seeds of the *bzr1* mutant and Nip treated with GA, PAC, or ethanol (mock). Error bars represent SD (n = 3 experiments, each replicate contained 30 seeds). *$P < 0.05$; **$P < 0.01$ (Student's t test). The images were digitally extracted for comparison in (E).

increased transient starch granule accumulation is negatively correlated with shoot growth. Furthermore, it was obvious that more starch granules accumulated in each side of *d61* shoots compared to their counterparts in the wild-type (Figure 6, A–G). Similar phenomena were observed in the *bzr1-i1* mutant and its wild-type (Figure 6, H–N). Moreover,

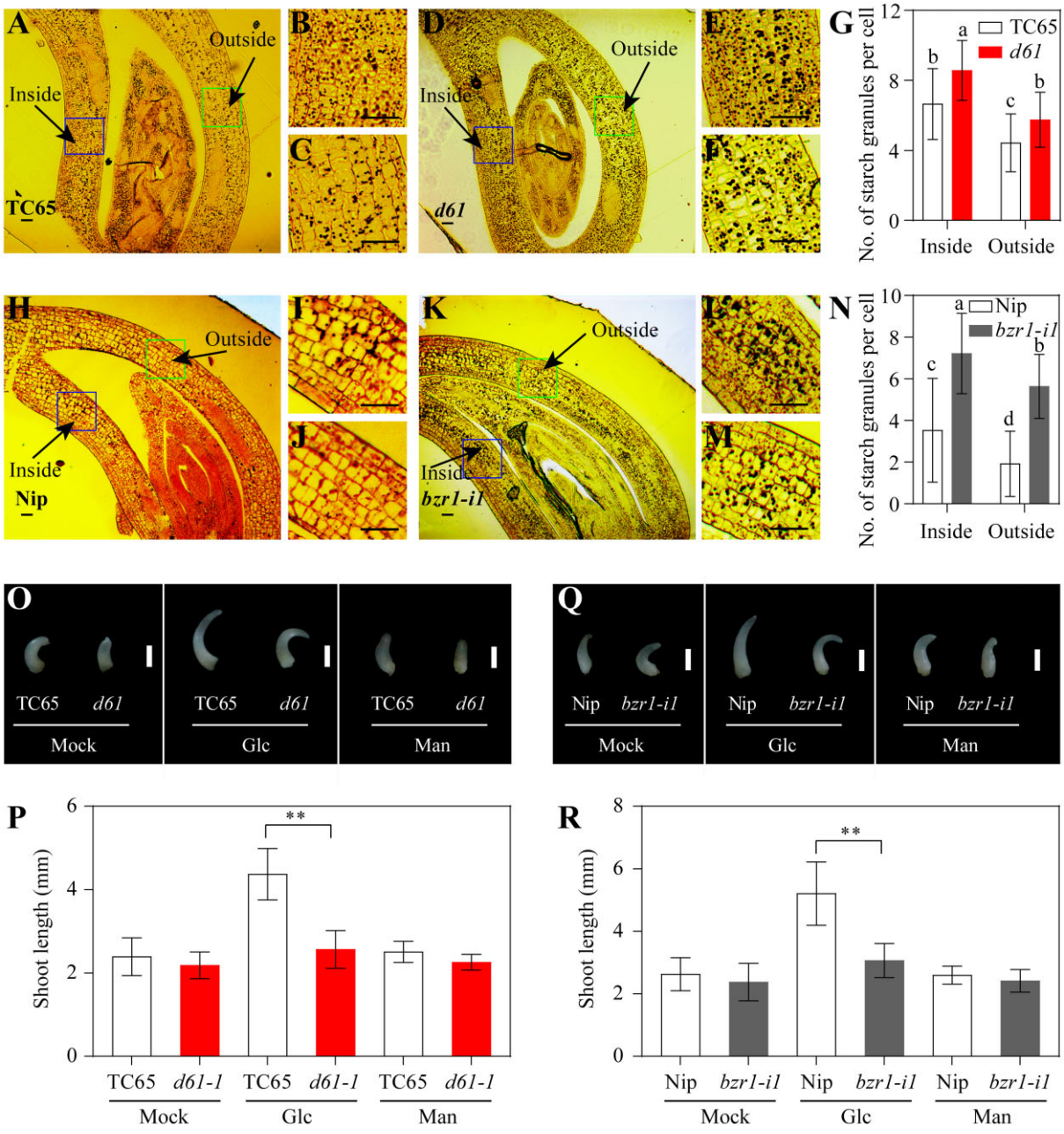

Figure 6 The BZR1-*RAmy3D* transcriptional module also plays essential roles in tissues of the embryo. A–F, Microscopic observation of starch granules that have accumulated in the shoots of Taichung 65 (TC65) (A–C) and *d61* (D–F) at 36 HAI. The samples were embedded in LR white resin, cut into semi-thin sections, and stained with iodine solution. (B) and (C) are enlargements of the rectangles marked with blue boxes on the inside parts and green boxes on the outside parts of the shoots in (A), respectively. E and F are enlargements of the rectangles marked with blue boxes on the inside parts and green boxes on the outside parts of the shoots in (D), respectively. Scale bar = 20 μm. G, Statistical analysis of the average number of starch granules per cell in shoots of the *d61* mutant and TC65 control. H–M, Microscopic observation of the starch granules that have accumulated in the shoots of Nip (H–J) and the *bzr1-i1* mutant (K–M) at 36 HAI. I and J are the enlargements of the rectangles marked with blue boxes on the inside parts and green boxes in the outside parts of the shoots in (H), respectively. L and M are the enlargements of the rectangles marked with blue boxes on the inside parts and green boxes on the outside parts of the shoots in (K), respectively. N, Statistical analysis of the average number of starch granules per cell in shoots of the *bzr1-i1* mutant and Nip control. In (G) and (N), error bars represent SD (n = 3 experiments, each replicate contained 30 cells). Different letters indicate significant differences at $P < 0.05$ by Duncan's multiple range test. O and P, Morphology (O) and quantitative analysis (P) of the plumule lengths in the *d61* mutant and TC65 control cultivated in vitro for 120 h supplemented with Glc or Man or the mock control. Q and R, Morphology (Q) and quantitative analysis (R) of the plumules length in the *bzr1-i1* mutant and Nip control cultivated in vitro for 120 h supplemented with Glc or Man or mock. Glc, glucose; Man, mannitol. Scale bar = 1 mm. Error bars represent SD (n = 3 experiments, each replicate contained 20 plumules). $^{**}P < 0.01$ (Student's t test). The images were digitally extracted for comparison in (O) and (Q).

the general cell size in both the *d61* and *bzr1-i1* mutants was smaller than that in their respective wild-types (Supplemental Figure S14), which is consistent with previous reports in Arabidopsis (Zhong et al., 2021).

To verify whether the BZR1-*RAmy3D* module also functions in the embryo tissues, we first performed reverse transcription quantitative polymerase chain reaction (RT-qPCR). The results showed that *RAmy3D* expression is notably decreased in *d61* and *bzr1-i1* plumules compared to their respective wild-type controls (Supplemental Figure S15). To further clarify this observation and to eliminate potential interference from the endosperm (the different glucose flow from degraded starch in various endosperm sources, for example), the in vitro embryogenic culture system was used. In this assay, isolated embryos were cultured in vitro. The results indicated that the shoot lengths of the *d61* and *bzr1-i1* mutants showed no significant differences from their respective wild-types when cultured with water only (Figure 6, O–R). However, in the presence of glucose, the shoot lengths of the wild-types markedly increased, while shoot lengths of the *d61* and *bzr1-i1* mutants showed no significant change (Figure 6, O–R). We used the same concentration of mannitol to rule out the possibility that the effect on shoot growth resulted from osmotic pressure (Figure 6, O–R). In summary, blocking BR signaling attenuated BZR1 activity and *RAmy3D* expression, thus triggering the slower degradation of transient starch in embryo cells and the consequent inhibition of embryo growth.

Transcriptome profile of BZR1-responsive genes during seed germination via RNA-seq

To explore other BZR1-responsive targets involved in regulating rice germination, an RNA-seq experiment was performed using the *BZR1-OX2* line. A total of 1,682 differentially expressed genes (DEGs) were identified in the *BZR1-OX2* line (fold change >1.5, adjusted $P<0.05$), including 228 upregulated and 1,634 downregulated genes (Supplemental Figure S16A). Not surprisingly, both *OsBZR1* and *RAmy3D* were in the list of upregulated genes (Supplemental Table S1). Based on the Kyoto Encyclopedia of Genes and Genomes (KEGG) analysis, the five most enriched pathways of the DEGs included "phenylpropanoid biosynthesis", "plant hormone signal transduction", "plant–pathogen interaction", "starch and sucrose metabolism", and "fatty acid elongation" (Supplemental Figure S16B). We then randomly selected four genes from each group of DEGs to verify the RNA-seq results. RT-qPCR assays showed that the expression changes in these genes in the *BZR1-OX2* line were the same as determined by the RNA-seq data, while seven out of the eight genes showed the opposite changes in expression in the *bzr1* mutant compared to *BZR1-OX2* (Figure 7, A and B), suggesting that the RNA-seq data is credible.

All our data demonstrate that the BZR1-*RAmy3D* transcriptional module functions in both the rice endosperm and embryo to accelerate seed germination and post-germination growth (Figure 8).

Discussion

BR promotes seed germination and post-germination growth

Seed germination is closely correlated to robust and healthy seedling development, and hence influences the final crop yield. BR plays multiple roles in controlling a number of important agronomic traits in rice, including plant height, leaf angle, grain filling, grain shape, stress resistance, and seed germination. The BR-insensitive rice mutant *d61*, which has a mutation in the receptor BRI1, has shorter coleoptile and root lengths when germinated in the dark (Yamamuro et al., 2000), which is consistent with our data (Figure 1, A and B; Supplemental Figure S2). Moreover, *d61* and the *OsGSK2* overexpression line had shorter mesocotyl lengths, while *OsGSK2-RNAi* had longer mesocotyls (Sun et al., 2018). Furthermore, we also analyzed seed germination in several BR signaling mutants or transgenic rice lines. The results showed that the germination of *d61*, *Go*, and *bzr1* rice seeds is similar, with delayed germination and shorter shoot length than their respective controls, while modulation of *DLT* had no observable effect on seed germination (Figures 1, 2, H and I). These results suggest that BR signaling regulates seed germination and post-germination growth via the BRI1-GSK2-BZR1 signaling cascade.

BZR1 enhances starch mobilization by promoting *RAmy3D* expression

Seed dormancy and germination are tightly controlled by multiple exogenous and endogenous stimuli (Finkelstein et al., 2008; SHu et al., 2016; Yang et al., 2020). Although a number of new mechanisms involved in seed germination have been discovered, such as post-translational modifications, RNA-binding protein, microRNAs, and alternative splicing, they are all directly or indirectly correlated to the mobilization of seed storage reserves (Müntz et al., 2001; Xue et al., 2021; Yu et al., 2021). In general, seed germination follows a classic triphasic model, and phase II is the most important stage during which all the metabolic reactions required by germination are reactivated, including starch hydrolysis and storage protein degradation (He and Yang, 2013). Although storage reserve degradation affects seed germination, the detailed regulatory mechanisms are still unclear. Our previous study showed that BR and GA coregulate seed germination and embryo growth by modulating glutelin mobilization (Xiong et al., 2021). Starch is the most abundant component of the endosperm, accounting for 90% of the dry weight. Since the breakdown of starch into sugar provides substrates for rice embryo growth, the rate of degradation affects the germination speed. The slower consumption of starch and less soluble sugar production in TRS (a line with high resistant starch) endosperm delays seed germination (Pan et al., 2018). In maize, the coleoptile length of the *starch branching enzyme 1a* (*sbe1a*)

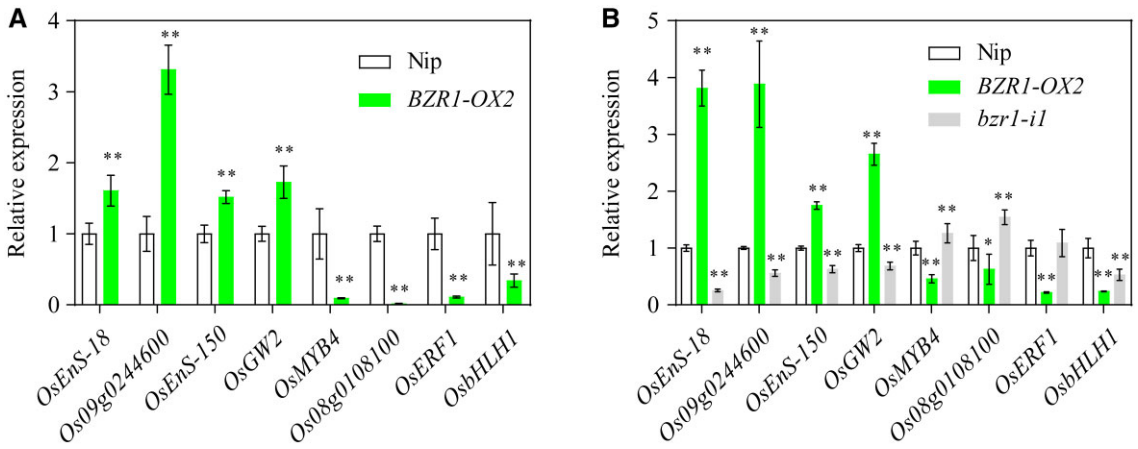

Figure 7 Validation of RNA-seq data for the representative target genes by RT-qPCR. A, RNA-seq data of eight representative DEGs in *BZR1-OX2* seeds at 2 HAI. The gene expression levels in Nip were set to 1. B, Verification of the DEGs by RT-qPCR in both *BZR1-OX2* and *bzr1-i1* mutant seeds at 2 HAI. The gene expression levels in Nip were set to 1. *Actin1* was used as the internal control for normalization of gene expression. Error bars represent SD (n = 3 experiments, each replicate contained 30 seeds). *$P < 0.05$; **$P < 0.01$ (Student's t test).

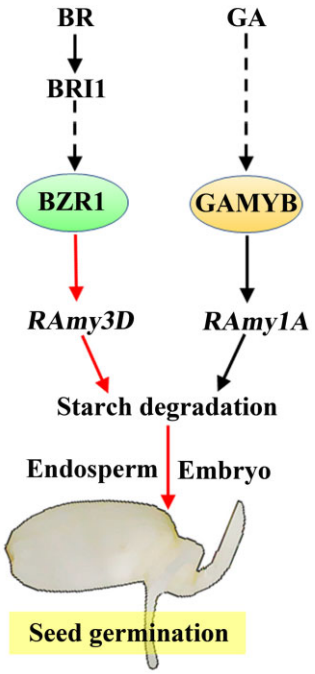

Figure 8 Working model for the BZR1-mediated transcriptional module in the regulation of rice seed germination. BR promotes germination in rice seeds via the key transcription factor BZR1 that mediates the expression of downstream target genes. One representative direct target of BZR1 is *RAmy3D*, a gene that encodes an important α-amylase that plays a crucial role in starch degradation at the initial stage of seed germination. The BZR1-*RAmy3D* transcriptional module, which is independent of the GAMYB-*RAmy1A* module, functions in both the endosperm and in embryo-related tissues. Moreover, both RAmy3D and RAmy1A promote starch turnover, thus providing more sugars for seed germination and embryo growth. Broken lines indicate indirect or multistep regulation. Arrowheads represent positive regulation.

mutant is reduced because more starch remains in the seeds during germination (Xia et al., 2011). Due to a mutation in *Isoamylase 1* (*ISA1*), the *preharvest sprouting 8* (*phs8*) rice mutant accumulates more sugar in the endosperm, which leads to the PHS phenotype (Du et al., 2018). These studies demonstrate a positive correlation between starch degradation and seed germination. In the present study, we have shown that blocking BR signaling can suppress α-amylase expression and activity (Figure 3; Supplemental Figure S6), thus delaying starch degradation (Supplemental Figure S7) and reducing the soluble sugar content (Supplemental Figure S8), and consequently inhibiting seed germination (Figure 2, H and I).

BZR1 is a key transcription factor that mediates the regulatory effect of BR on plant growth and development by directly binding to various downstream target genes. For example, BZR1 also promotes accumulation of *OsmiR396d*, which negatively regulates the expression of the rice growth-regulating factors *4* (*OsGRF4*) and *OsGRF6* that regulate leaf angle and plant height, respectively (Tang et al., 2018). In addition, BZR1 directly suppresses the expression of the *aldehyde dehydrogenase* (*OsALDH2B1*) and *allene oxide synthase* (*AOS2*) genes to regulate the jasmonic acid pathway, thus modulating the growth-defense tradeoff in rice (Ke et al., 2020). In this study, we successfully identified *RAmy3D* as a reliable direct target of BZR1 (Figure 4). *RAmy3D* encodes an α-amylase with positive roles in controlling seed germination (Lu et al., 2007). The overexpression of *RAmy3D* promotes rice germination under normal conditions, which could be further enhanced in response to abiotic stress (Chen et al., 2019). In addition, our RNA-seq data also demonstrated that OsBZR1 can modulate the starch and sucrose metabolic pathways during seed germination (Supplemental Figure S16B).

The BZR1-*RAmy3D* module is essential for regulating seed germination by enhancing starch mobilization in both the rice embryo and endosperm

Our study identified a novel BR-regulated molecular cascade that modulates *RAmy3D* expression and starch degradation

in rice. BZR1 binds directly to the E-box in the *RAmy3D* promoter and positively regulates its expression (Figure 4), thus increasing α-amylase activity and soluble sugar content (Figure 3; Supplemental Figure S8). Therefore, the BZR1-*RAmy3D* module functions in the rice endosperm to regulate storage starch degradation, which provides soluble sugars for embryo growth. However, it is still mostly unknown what happens after the sugars are transported into the embryo. A previous study showed that *RAmy3D* is expressed in both the embryo and aleurone during seed germination (Karrer et al., 1991). Transient starch will then be newly synthesized and will accumulate in the vascular tissue of the embryo when sufficient sugar is provided (Matsukura et al., 2000). In addition, more starch grains were observed in shoots of the GA-deficient mutant *osko1* (*ent-kaurene oxidase 1*), leading to slower germination (Zhang et al., 2020). Interestingly, we also observed a similar transient starch accumulation phenotype in the BR insensitive mutants *d61* and *bzr1* (Figure 6, A–N). Moreover, the transient starch accumulation was unequal even within the same tissue, and regions with more starch granules had smaller cells (Figure 6, A–N; Supplemental Figure S14). This implies that the number of starch granules in the plumule cells is negatively correlated with starch mobilization efficiency and, consequently, cell size. When BR signaling is blocked, the stability and activity of BZR1 are attenuated (Li et al., 2012, 2018a), thus leads to decreased expression of *RAmy3D* and increased starch granules in the embryo (Supplemental Figure S15). The in vitro plumule elongation assay is useful to eliminate the different sugar flow from the endosperm, and it further demonstrated that the embryo also requires an intact BR signaling pathway to utilize glucose and promote embryo growth (Figure 6, O–R).

Furthermore, *RAmy1A*, another α-amylase gene, also plays crucial roles in promoting seed germination (Asatsuma et al., 2005). *RAmy1A* expression is directly induced by the transcription factor GAMYB (Washio, 2003). Our study clarified that the newly established BZR1-*RAmy3D* module is independent of the previously described GAMYB-*RAmy1A* module. First, the *RAmy3D* expression pattern is quite different from that of *RAmy1A* during the course of seed germination (Supplemental Figures S10 and S13). Second, BZR1 binds specifically only to the *RAmy3D* promoter, not the *RAmy1A* promoter (Figures 4 and 5A). The situation is opposite to that of GAMYB (Figures 4, C and 5, A–C). Finally, the germination speed and shoot length in the *bzr1* mutant were further decreased in response to PAC treatment (Figure 5, E–G). Although the BZR1-*RAmy3D* and GAMYB-*RAmy1A* modules are relatively independent, crosstalk between BR and GA does exist. GA recovers germination in seeds deficient in BR biosynthesis by modulating glutelin mobilization (Li et al., 2020). When the BR concentration is low in rice, *BZR1* promotes GA biosynthesis and subsequent cell elongation. However, when the BR concentration is high, the inhibitory feedback regulation of both BR and GA biosynthesis mediated by *BZR1* is activated (Tong and Chu, 2018).

bzr1 can be used to prevent PHS

BR is considered to be a potential biotechnological target for enhancing crop yield and stress tolerance (Divi and Krishna, 2009; Gruszka et al., 2021). However, the pleiotropic effects of BR hinder its wide application in crop breeding programs (Khripach et al., 2000). For instance, direct modulation of BR biosynthesis or signaling will affect a series of agronomic traits in rice (Tong and Chu, 2018). Therefore, the dissection of downstream specific transcription factors or BR-responsive target genes will facilitate the application of BR in crop breeding with few adverse effects. At present, due to the decrease in arable agricultural land and the increased demand for food, breeding rice with compact plant architecture for dense planting is a feasible strategy to reduce the competition for water, light, and nutrients (Sakamoto et al., 2006). In maize, knocking down *Related to ABI3/VP1-Like 1* (*ZmRAVL1*), a gene regulating BR biosynthesis, changed the endogenous BR content and the leaf angle, which increased yield at high density planting (Tian et al., 2019). In rice, the yield of the densely planted BR-deficient mutant *osdwarf4-1* with erect leaves was 32.0% higher than that of the wild-type under conventional planting (Sakamoto et al., 2006). Moreover, although the 1,000-grain weight of *d61-7*, a weak *BRI1* mutant, was about 21% lower than in wild-type, the yield was almost the same as that of wild-type under high-density planting (Morinaka et al., 2006). In the present study, knocking out *OsBZR1* led to plants with compact architecture that were slightly reduced in height (Figure 2, F and G; Supplemental Figure S3, A and B), traits that meet the requirements of modern crop breeding programs. Although the 1,000-grain weight of the *bzr1-i1* and *bzr1-d4* mutants decreased by 8.4% and 6.9%, respectively (Supplemental Figure S3G), they have the potential to produce higher yields under appropriately dense planting conditions. Most importantly, PHS in the *bzr1* mutants was notably lower than in the wild-type control, which will prevent great losses in rice yield and grain quality.

Materials and methods

Plant materials, growth conditions, and agronomic trait analysis

A number of BR-related rice materials (*O. sativa* ssp. *japonica*) were used in this study, including *d61* and its wild-type TC65 (Yamamuro et al., 2000), *Go*, *dlt*, *Do*, and their wild-type ZH11 (Tong et al., 2012), *BZR1-OX*, *bzr1*, and their wild-type Nip. *BZR1-OX* and *bzr1* are *BZR1* overexpression and knockout mutant rice lines, respectively, which were generated in our laboratory. In brief, various BR signaling mutants are produced in different recipient rice varieties. Therefore, specific wild-type should be chosen and taken as control for corresponding BR signaling mutant in various experiments.

All rice plants were grown under the same climatic and management conditions during the summer in a paddy field

at Yangzhou University (Yangzhou, Jiangsu province, China). At seed maturity, plant height and 1,000-grain weight were measured. Mature seeds from superior spikelets were collected for analysis of grain size and seed germination.

Transgene constructs and rice transformation

To construct the *BZR1*-OX vector, the *BZR1* coding sequence (CDS) was cloned into the plant binary vector *pCAMBIA1300* under control of the *OsActin* promoter and fused to the 3 × *FLAG* epitope. To create the CRISPR/Cas9 gene editing vectors, the specific target site for *BZR1* was designed and cloned into the *pC1300-Cas9* vector (Shen et al., 2017; Xie et al., 2017). The verified constructs were then transferred into the *japonica* rice cultivars "Nip" via *Agrobacterium tumefaciens*-mediated transformation. All primers used here are listed in Supplemental Table S2.

Analysis of seed germination and in vitro embryo culture

The procedure for germination analysis has been described previously (Li et al., 2020). Seeds with a radicle >1 mm in length were considered to have successfully germinated (Cheng et al., 2013).

The method for in vitro culture of rice embryos was described previously (Xiong et al., 2021). In brief, the isolated embryos were cultured in 100-mM glucose or mannitol solution. Five days later, the shoot lengths were measured using ImageJ software.

To evaluate the level of PHS of *BZR1*-related materials, five superior rice panicles were collected, immersed in water, and incubated at 30°C under a 14-h/10-h light/dark cycle (Liao et al., 2018). The number of germinated seeds was counted and recorded every 2 d.

Lamina joint inclination assay

The lamina joint test was performed following a well-established procedure (Li et al., 2018b). After floating on distilled water for 24 h, the entire segments consisting of 1 cm of leaf blade and sheath were incubated in 2.5-mM maleic acid potassium solution containing 1-μM BL or dimethyl sulfoxide (DMSO; mock) for 48 h in the dark. The angles of 20 samples were then measured for each treatment.

Analysis of soluble sugar and total starch contents

The anthrone-H_2SO_4 colorimetric method was used to determine the soluble sugar content of the germinated seeds. The method is described in detail in Pan et al. (2018).

Total starch content of rice seeds was determined by using Megazyme Total Starch Assay Kit (K-TSTA). The detailed procedure follows the protocol of the kit.

Qualitative and quantitative analysis of seed α-amylase activity

To qualitatively evaluate the α-amylase activity of BR-related materials during germination, we used the starch plate test following the method of Liu et al. (2018) with slight modifications. The rice seeds were first sterilized with 70% (v/v) ethanol for 15 min and then washed twice with Milli-Q water. Next, the embryo-less half-seeds were placed on 2% (w/v) agar in Petri dishes with the cut face in tight contact with the agar. Instead of potato starch, rice starch was used here since it is the actual substrate of α-amylase in rice seeds. After incubation at 28°C for 4 d in the dark, the starch plate was soaked in iodine solution, 0.1% I_2 (w/v) and 1% KI (w/v), for 5 min. Colorless halos around the half seeds form as a result of starch hydrolysis by α-amylase. The halo size is positively correlated with α-amylase activity.

Furthermore, the α-amylase activity was quantified using a colorimetric α-amylase test kit (Comin, Suzhou, Jiangsu, China). The major principle behind the kit assay is that amylase catalyzes starch hydrolysis into reducing sugars, and reducing sugars can change 3,5-dinitrosalicylic acid into a brown-red substance, which can then be measured by a UV–visible spectrophotometer.

RNA extraction, RT-qPCR assays, and RNA-Seq analysis

Total RNA was extracted from germinated seeds using the RNAprep pure Plant Kit (Tiangen, Beijing, China). Two-micrograms total RNA from each sample were pretreated with DNase I and used for reverse transcription. RT-qPCR was performed on a MyiQ real-time system (Bio-Rad, California, USA) with ChamQ Universal SYBR qPCR Master Mix (Vazyme Biotech, Jiangsu, China). *OsActin1* was used as the internal reference for normalization. Three biological replicates were included for each sample, and the primer information is shown in Supplemental Table S2. Seeds germinated for 2 h were used for RNA-seq analysis as described by Zhu et al. (2021).

Western blotting

For BRZ treatment, the 5-d-old rice seedlings were grown in water supplied with BRZ (2 μM) or its mock DMSO for 5 d. For BL treatment, the leaves of 10-d-old rice seedlings were cultured in water containing BL (1 μM) or DMSO for 3 h. The samples were then collected and ground into powder in liquid nitrogen.

Total protein was extracted from rice leaf samples and heated at 95°C for 10 min, and separated by denaturing polyacrylamide gel electrophoresis (SDS–PAGE). After electrophoresis, the proteins were transferred to a poly(vinylidene fluoride) membrane and then immunodetected with antibodies recognizing the FLAG tag (F3165, Sigma-Aldrich) or heat shock protein (BPI; http://www.proteomics.org.cn).

ChIP-qPCR assay

The ChIP assay was performed following the published protocol of Saleh et al. (2008) with minor modifications. In brief, young panicles of *BZR1-OX* rice plants were fully ground into a powder with liquid nitrogen and suspended in buffer. After protein–DNA cross-linking with formaldehyde, the nuclei were isolated and the chromatin DNA was broken into 200- to 1,000-bp fragments by sonication. The DNA–protein complexes were immunoprecipitated with an

anti-FLAG monoclonal antibody (1:200) and enriched using immunomagnetic beads. The collected complexes were decrosslinked to release the DNA fragments which were used for subsequent qPCR analysis following purification.

ChIP-qPCR was performed as described previously (Tong et al., 2014). A region of the *Actin1* intron was used for expression normalization, and a part of the 3′-untranslated region of the *GA2ox-3* gene was used as the negative control. Each DNA region test was repeated three times. The primers used are shown in Supplemental Table S2.

Dual-luciferase reporter assay

The Agrobacterium-mediated transient assay system was used to co-express the reporter and effector constructs in *Nicotiana benthamiana* leaf epidermal cells (Zhu et al., 2021). To generate reporter constructs, 2-kb promoter regions upstream of the *RAmy1A* and *RAmy3D* genes were individually cloned to generate effector constructs, and the CDSs of *OsBZR1* and *OsGAMYB* were each cloned into the *pGreenII 62-SK* reporter vector. Both a reporter and an effector construct were then introduced together into *N. benthamiana* leaves by agroinfiltration. Forty hours later, the infiltrated leaves were used for transcriptional activity assays. The firefly and *Renilla* luciferase signals were examined using the Dual Luciferase Reporter Assay Kit (Vazyme, Jiangsu, China).

EMSA

The *OsBZR1* CDS was cloned to generate the *MBP–BZR1* fusion gene. The MBP–BZR1 recombinant protein was then induced with 0.5-mM IPTG in *Escherichia coli* strain BL21 and purified using the PurKine MBP-Tag Protein Purification Kit (Abbkine, Hubei, China). The probe was labeled with biotin using the DNA 3′-End Biotinylation Kit (Thermo Scientific). The unlabeled probe was used as the competitor. The detailed procedure is described in Wu et al. (2019).

Yeast two-hybrid assay

The CDSs of *OsBZR1* and *OsGAMYB* were cloned into the pGBKT7 (BD) and pGADT7 (AD) vectors, respectively. The *BZR1-BD* and *GAMYB-AD* plasmids were then co-transformed into the yeast (*Saccharomyces cerevisiae*) strain AH109 and the positive transformants were then screened for protein–protein interactions.

Sectioning and iodine staining shoots of germinating seeds

The shoots of germinating seeds 36 HAI were harvested and immediately fixed in a solution consisting of 0.1-M Na-phosphate buffer and 2.5% glutaraldehyde. The fixed samples were soaked in phosphate buffer, dehydrated in an ethanol series, and then embedded in LR white resin. The samples were cut into 1.8-μm semithin sections using a Leica Ultrathin Microtome (EM UC7). Finally, the sections were stained with iodine solution, 0.1% I_2 (w/v) and 1% KI (w/v), and observed for the presence of starch.

Statistical analysis

In this study, most statistics were presented as mean ± SD. For experiments with single pairwise comparisons, Student's *t* test was used to determine the level of significance (*$P < 0.05$, **$P < 0.01$). For experiments with multiple comparisons, the data were analyzed with Duncan's multiple range test at $P < 0.05$ (with different letters).

Accession numbers

Genes sequence information in this study could be found in the Rice Annotation Project Database (RAP-DB) (https://rapdb.dna.affrc.go.jp/) under the following accession numbers: *OsBZR1* (Os07g0580500), *RAmy1A* (Os02g0765600), *RAmy1B* (Os01g0357400), *RAmy1C* (Os02g0765400), *RAmy2A* (Os06g0713800), *RAmy3A* (Os09g0457400), *RAmy3B* (Os09g0457600), *RAmy3C* (Os09g0457800), *RAmy3D* (Os08g0473900), *RAmy3E* (Os08g0473600), *GAMYB* (Os01g0812000), *GA2ox-3* (Os01g0757200), *OsEnS-18* (Os01g0805400), *OsEns-150* (Os12g0464400), *OsGW2* (Os02g0244100), *OsMYB4* (Os04g0517100), *OsERF1* (Os04g0546800), *OsbHLH1* (Os01g0928000).

Supplemental data

The following materials are available in the online version of this article.

Supplemental Figure S1. Phenotypes of BR-insensitive mutants and their corresponding wild-types, including *d61* and Taichung 65 (TC65), *Go*, *Do*, *dlt*, and Zhonghua 11 (ZH11).

Supplemental Figure S2. Morphological changes in seeds of BR-insensitive mutants at 96 HAI.

Supplemental Figure S3. Phenotypes of *BZR1*-related rice mutants and overexpression transgenic lines.

Supplemental Figure S4. Plant height in the 2-week old rice seedlings.

Supplemental Figure S5. Morphological changes in seeds of *BZR1-OX*, *bzr1-i1*, and wild-type Nip at 96 HAI.

Supplemental Figure S6. Analysis of α-amylase activity in *BZR1-OX2*, *bzr1-i1*, and wild-type Nip seeds.

Supplemental Figure S7. Starch contents of germinating seeds of BR-related rice lines and the corresponding wild-type controls at 2 HAI and 96 HAI.

Supplemental Figure S8. Soluble sugar contents of germinating seeds of BR-related rice lines and the corresponding wild-type controls at 2 HAI and 96 HAI.

Supplemental Figure S9. Analysis of the expression pattern of *BZR1* in germinating rice seeds from 2 to 96 HAI.

Supplemental Figure S10. Analysis of the expression pattern of *RAmy3D* in germinating rice seeds from 2 to 96 HAI.

Supplemental Figure S11. Schematic maps of the reporter and effector constructs used in the dual-luciferase reporter assay.

Supplemental Figure S12. The OsBZR1 protein binds to the P3 region of the promoter as shown by EMSA.

Supplemental Figure S13. Analysis of *RAmy1A* expression in germinating rice seeds from 2 to 96 HAI.

Supplemental Figure S14. Quantitative data of the length and width of cells in the shoots of *d61*, *bzr1-i1* mutants and the corresponding wild-type controls.

Supplemental Figure S15. RT-qPCR analysis of *RAmy3D* expression in embryos of *d61*, *bzr1-i1* and their corresponding wild-types at 6 HAI.

Supplemental Figure S16. Transcriptomic analysis of *BZR1-OX* transgenic rice seeds.

Supplemental Table S1. The DEGs in *BZR1-OX2* transgenic rice compared to WT by RNA-seq.

Supplemental Table S2. Primers used in this study.

Acknowledgments

We thank H.N. Tong (Institute of Crop Sciences, Chinese Academy of Agricultural Sciences) and C.C. Chu (Institute of Genetics and Developmental Biology, Chinese Academy of Sciences) for providing the *dlt* mutant as well as *Go* and *Do* transgenic rice.

Funding

This work was supported by the National Natural Science Foundation of China (31825019, 32071984), Science Fund for Distinguished Young Scholars of Jiangsu Province (BK20200045), Jiangsu Six Talent Peaks (SWYY-154), other programs from Jiangsu Province Government (PAPD, Qinglan, and "333").

Conflict of interest statement. None declared.

References

Andriotis VM, Rejzek M, Rugen MD, Svensson B, Smith AM, Field RA (2016) Iminosugar inhibitors of carbohydrate-active enzymes that underpin cereal grain germination and endosperm metabolism. Biochem Soc Trans **44:** 159–165

Asatsuma S, Sawada C, Itoh K, Okito M, Kitajima A, Mitsui T (2005) Involvement of α-amylase I-1 in starch degradation in rice chloroplasts. Plant Cell Physiol **46:** 858–869

Bai M, Zhang L, Gampala SS, Zhu S, Song W, Chong K, Wang, Z (2007) Functions of OsBZR1 and 14-3-3 proteins in brassinosteroid signaling in rice. Proc Natl Acad Sci USA **104:** 13839–13844

Chen PW, Chiang CM, Tseng TH, Yu SM (2006) Interaction between rice MYBGA and the gibberellin response element controls tissue-specific sugar sensitivity of α-amylase genes. Plant Cell **18:** 2326–2340

Chen YS, Ho TD, Liu L, Lee DH, Lee CH, Chen YR, Lin SY, Lu CA, Yu SM (2019) Sugar starvation-regulated MYBS2 and 14-3-3 protein interactions enhance plant growth, stress tolerance, and grain weight in rice. Proc Natl Acad Sci USA **116:** 21925–21935

Cheng X, Wu Y, Guo J, Du B, Chen R, Zhu L, He G (2013) A rice lectin receptor-like kinase that is involved in innate immune responses also contributes to seed germination. Plant J **76:** 687–698

Damaris RN, Lin Z, Yang P, He D (2019) The rice alpha-amylase, conserved regulator of seed maturation and germination. Int J Mol Sci **20:** 450

Divi UK, Krishna P (2009) Brassinosteroid: a biotechnological target for enhancing crop yield and stress tolerance. New Biotechnol **26:** 131–136

Du L, Xu F, Fang J, Gao S, Tang J, Fang S, Wang H, Tong H, Zhang F, Chu J, et al. (2018) Endosperm sugar accumulation caused by mutation of *PHS8/ISA1* leads to pre-harvest sprouting in rice. Plant J **95:** 545–556

Finkelstein R, Reeves W, Ariizumi T, Steber C (2008) Molecular aspects of seed dormancy. Annu Rev Plant Biol **59:** 387–415

Gómez A, Zentella R, Walker MK, Ho TH (2001) Gibberellin/abscisic acid antagonism in barley aleurone cells: site of action of the protein kinase PKABA1 in relation to gibberellin signaling molecules. Plant Cell **13:** 667–679

Gruszka D, Bajguz A, Li QF, Hayat S, Hansson M, Wang XL, Li JM (2021) An update on brassinosteroids: homeostasis, crosstalk, and adaptation to environmental stress. Front Plant Sci **12:** 677

Gubler F, Jacobsen JV (1992) Gibberellin-responsive elements in the promoter of a barley high-pI alpha-amylase gene. Plant Cell **4:** 1435–1441

He DL, Yang PF (2013) Proteomics of rice seed germination. Front Plant Sci **4:** 246

He JX, Gendron JM, Sun Y, Gampala SS, Gendron N, Sun CQ, Wang ZY (2005) BZR1 is a transcriptional repressor with dual roles in brassinosteroid homeostasis and growth responses. Science **307:** 1634–1638

Holdsworth MJ, Bentsink L, Soppe WJ (2008) Molecular networks regulating Arabidopsis seed maturation, after-ripening, dormancy and germination. New Phytol **179:** 33–54

Hong YF, Ho TH, Wu CF, Ho SL, Yeh RH, Lu CA, Chen PW, Yu LC, Chao A, Yu SM (2012) Convergent starvation signals and hormone crosstalk in regulating nutrient mobilization upon germination in cereals. Plant Cell **24:** 2857–2873

Hu Q, Fu Y, Guan Y, Lin C, Cao D, Hu W, Sheteiwy M, Hu J (2016) Inhibitory effect of chemical combinations on seed germination and pre-harvest sprouting in hybrid rice. Plant Growth Regul **80:** 281–289

Hu Y, Yu D (2014) BRASSINOSTEROID INSENSITIVE2 interacts with ABSCISIC ACID INSENSITIVE5 to mediate the antagonism of brassinosteroids to abscisic acid during seed germination in *Arabidopsis*. Plant Cell **26:** 4394–4408

Huang N, Stebbins GL, Rodriguez RL (1992) Classification and evolution of alpha-amylase genes in plants. Proc Natl Acad Sci USA **89:** 7526–7530

Hwang YS, Thomas B, Rodriguez R (1999) Differential expression of rice α-amylase genes during seedling development under anoxia. Plant Mol. Biol **40:** 911–920

Karrer EE, Litts JC., Rodriguez RL (1991) Differential expression of α-amylase genes in germinating rice and barley seeds. Plant Mol Biol **16:** 797–805

Karrer EE, Chandler JM, Foolad MR, Rodriguez RL (1992) Correlation between α-amylase gene expression and seedling vigor in rice. Euphytica **66:** 163–169

Ke Y, Yuan M, Liu H, Hui S, Qin X, Chen J, Zhang Q, Li X, Xiao J, Zhang Q, et al. (2020) The versatile functions of OsALDH2B1 provide a genic basis for growth–defense trade-offs in rice. Proc Natl Acad Sci USA **117:** 3867–3873

Khripach V, Zhabinskii V, Groot A (2000) Twenty years of brassinosteroids: steroidal plant hormones warrant better crops for the XXI century. Ann Bot **86:** 441–447

Lanahan MB, Ho T, Rogers SW, Rogers JC (1992) A gibberellin response complex in cereal alpha-amylase gene promoters. Plant Cell **4:** 203–211

Li QF, Lu J, Yu JW, Zhang CQ, He JX, Liu QQ (2018a) The brassinosteroid-regulated transcription factors BZR1/BES1 function as a coordinator in multisignal-regulated plant growth. Biochim Biophys Acta Gene Regul Mech **1861:** 561–571

Li QF, Wang CM, Jiang L, Li S, Sun SS, He JX (2012) An interaction between BZR1 and DELLAs mediates direct signaling crosstalk between brassinosteroids and gibberellins in Arabidopsis. Sci Signal **5:** ra72

Li QF, Yu JW, Lu J, Fei HY, Luo M, Cao BW, Huang LC, Zhang CQ, Liu QQ (2018b) Seed-specific expression of *OsDWF4*, a rate-limiting gene involved in brassinosteroids biosynthesis,

improves both grain yield and quality in rice. J Agric Food Chem **66:** 3759–3772

Li QF, Zhou Y, Xiong M, Ren XY, Han L, Wang JD, Zhang CQ, Fan XL, Liu QQ (2020) Gibberellin recovers seed germination in rice with impaired brassinosteroid signalling. Plant Sci **293:** 110435

Liao Y, Bai Q, Xu P, Wu T, Guo D, Peng Y, Zhang H, Deng X, Chen X, Luo M, et al. (2018) Mutation in rice *abscisic acid2* results in cell death, enhanced disease-resistance, altered seed dormancy and development. Front Plant Sci **9:** 405

Liu L, Xia W, Li H, Zeng H, Wei B, Han S, Yin C (2018) Salinity inhibits rice seed germination by reducing α-amylase activity via decreased bioactive gibberellin content. Front Plant Sci **9:** 275

Lu CA, Lin CC, Lee KW, Chen JL, Huang LF, Ho SL, Liu HJ, Hsing YI, Yu SM (2007) The SnRK1A protein kinase plays a key role in sugar signaling during germination and seedling growth of rice. Plant Cell **19:** 2484–2499

Matsukura C, Saitoh T, Hirose T, Ohsugi R, Perata P, Yamaguchi J (2000) Sugar uptake and transport in rice embryo. Expression of companion cell-specific sucrose transporter (*OsSUT1*) induced by sugar and light. Plant Physiol **124:** 85–93

Morinaka Y, Sakamoto T, Inukai Y, Agetsuma M, Kitano H, Ashikari M, Matsuoka M (2006) Morphological alteration caused by brassinosteroid insensitivity increases the biomass and grain production of rice. Plant Physiol **141:** 924–931

Müntz K, Belozersky M, Dunaevsky Y, Schlereth A, Tiedemann J (2001) Stored proteinases and the initiation of storage protein mobilization in seeds during germination and seedling growth. J Exp Bot **52:** 1741–1752

Noronha H, Silva A, Dai Z, Gallusci P, Rombolà AD, Delrot S, Gerós H (2018) A molecular perspective on starch metabolism in woody tissues. Planta **248:** 559–568

Pan T, Lin L, Wang J, Liu Q, Wei C (2018) Long branch-chains of amylopectin with B-type crystallinity in rice seed with inhibition of starch branching enzyme I and IIb resist in situ degradation and inhibit plant growth during seedling development. BMC Plant Biol **18:** 1–11

Sakamoto T, Morinaka Y, Ohnishi T, Sunohara H, Fujioka S, Ueguchi-Tanaka M, Mizutani M, Sakata K, Takatsuto S, Yoshida S, et al. (2006). Erect leaves caused by brassinosteroid deficiency increase biomass production and grain yield in rice. Nat Biotechnol **24:** 105–109

Saleh A, Alvarez-Venegas R, Avramova Z (2008) An efficient chromatin immunoprecipitation (ChIP) protocol for studying histone modifications in Arabidopsis plants. Nat Protoc **3:** 1018

Scofield GN, Aoki N, Hirose T, Takano M, Jenkins CL, Furbank RT (2007) The role of the sucrose transporter, OsSUT1, in germination and early seedling growth and development of rice plants. J Exp Bot **58:** 483–495

Shen L, Hua YF, Fu YP, Li J, Liu Q, Jiao XZ, Xin GW, Wang JJ, Wang XC, Yan CJ, et al. (2017) Rapid generation of genetic diversity by multiplex CRISPR/Cas9 genome editing in rice. Sci China Life Sci **60:** 506–515

Shu K, Liu Xd, Xie Q, He ZH (2016) Two faces of one seed: hormonal regulation of dormancy and germination. Mol Plant **9:** 34–45

Sinclair TR, Sheehy JE (1999) Erect leaves and photosynthesis in rice. Science **283:** 1455

Sun S, Chen D, Li X, Qiao S, Shi C, Li C, Shen H, Wang X (2015) Brassinosteroid signaling regulates leaf erectness in *Oryza sativa* via the control of a specific U-type cyclin and cell proliferation. Dev Cell **34:** 220–228

Sun S, Wang T, Wang L, Li X, Jia Y, Liu C, Huang X, Xie W, Wang X (2018) Natural selection of a GSK3 determines rice mesocotyl domestication by coordinating strigolactone and brassinosteroid signaling. Nat Commun **9:** 1–13

Tang Y, Liu H, Guo S, Wang B, Li Z, Chong K, Xu Y (2018) OsmiR396d affects gibberellin and brassinosteroid signaling to regulate plant architecture in rice. Plant Physiol **176:** 946–959

Tian J, Wang C, Xia J, Wu L, Xu G, Wu W, Li D, Qin W, Han X, Chen Q, et al. (2019) Teosinte ligule allele narrows plant architecture and enhances high-density maize yields. Science **365:** 658–664.

Tong H, Chu C (2018) Functional specificities of brassinosteroid and potential utilization for crop improvement. Trends Plant Sci **23:** 1016–1028

Tong H, Jin Y, Liu W, Li F, Fang J, Yin Y, Qian Q, Zhu L, Chu C (2009) DWARF AND LOW-TILLERING, a new member of the GRAS family, plays positive roles in brassinosteroid signaling in rice. Plant J **58:** 803–816

Tong H, Liu L, Jin Y, Du L, Yin Y, Qian Q, Zhu L, Chu C (2012) DWARF AND LOW-TILLERING acts as a direct downstream target of a GSK3/SHAGGY-like kinase to mediate brassinosteroid responses in rice. Plant Cell **24:** 2562–2577

Tong H, Xiao Y, Liu D, Gao S, Liu L, Yin Y, Jin Y, Qian Q, Chu C (2014) Brassinosteroid regulates cell elongation by modulating gibberellin metabolism in rice. Plant Cell **26:** 4376–4393

Washio K (2003) Functional dissections between GAMYB and Dof transcription factors suggest a role for protein-protein associations in the gibberellin-mediated expression of the RAmy1A gene in the rice aleurone. Plant Physiol **133:** 850–863

Wu CJ, Shan W, Liang SM, Zhu L, Guo YF, Chen JY, Lu WJ, Li QF, Su XG, Kuang JF (2019) MaMPK2 enhances MabZIP93-mediated transcriptional activation of cell wall modifying genes during banana fruit ripening. Plant Mol Biol **101:** 113–127

Xia H, Yandeau-Nelson M, Thompson DB, Guiltinan MJ (2011) Deficiency of maize starch-branching enzyme i results in altered starch fine structure, decreased digestibility and reduced coleoptile growth during germination. BMC Plant Biol **11:** 1–13

Xie XR, Ma XL, Zhu QL, Zeng DC, Li GS, Liu YG (2017) CRISPR-GE: a convenient software toolkit for CRISPR-based genome editing. Mol Plant **10:** 1246–1249

Xiong M, Chu L, Li Q, Yu J, Yang Y, Zhou P, Zhou Y, Zhang C, Fan X, Zhao D, et al. (2021) Brassinosteroid and gibberellin coordinate rice seed germination and embryo growth by regulating glutelin mobilization. Crop J **9:** 1039–1048

Xue XF, Jiao FC, Xu H., Jiao QQ, Zhang X, Zhang Y, Du SY, Xi MH, Wang A, Chen JT (2021) The role of RNA-binding protein, microRNA and alternative splicing in seed germination: a field need to be discovered. BMC Plant Biol **21:** 1–11

Yamamuro C, Ihara Y, Wu X, Noguchi T, Fujioka S, Takatsuto S, Ashikari M, Kitano H, Matsuoka M (2000) Loss of function of a rice brassinosteroid insensitive1 homolog prevents internode elongation and bending of the lamina joint. Plant Cell **12:** 1591–1605

Yang L, Liu S, Lin R (2020) The role of light in regulating seed dormancy and germination. J Integr Plant Biol **62:** 1310–1326

Yu F, Li M, He DL, Yang PF (2021) Advances on post-translational modifications involved in seed germination. Front Plant Sci **12**: 362

Zeeman SC, Kossmann J, Smith AM (2010) Starch: its metabolism, evolution, and biotechnological modification in plants. Annu Rev Plant Biol **61:** 209–234

Zhang H, Li M, He D, Wang K, Yang P (2020) Mutations on ent-kaurene oxidase 1 encoding gene attenuate its enzyme activity of catalyzing the reaction from ent-kaurene to ent-kaurenoic acid and lead to delayed germination in rice. PLos Genet **16:** e1008562

Zhang Q, Li C (2017) Comparisons of copy number, genomic structure, and conserved motifs for α-amylase genes from barley, rice, and wheat. Front Plant Sci **8:** 1727

Zhao X, Dou L, Gong Z, Wang X, Mao T (2019) BES1 hinders ABSCISIC ACID INSENSITIVE5 and promotes seed germination in *Arabidopsis*. New Phytol **221:** 908–918

Zhong C, Patra B, Tang Y, Li X, Yuan L, Wang X (2021) A transcriptional hub integrating gibberellin–brassinosteroid signals to promote seed germination in Arabidopsis. J Exp Bot **72:** 4708–4720

Zhu CC, Wang CX, Lu CY, Wang JD, Zhou Y, Xiong M, Zhang CQ, Liu QQ, Li QF (2021) Genome-wide identification and expression analysis of OsbZIP09 target genes in rice reveal its mechanism of controlling seed germination. Int J Mol Sci **22:** 1661